

Shape Complementarity Optimization of Antibody-Antigen Interfaces: the Application to SARS-CoV-2 Spike Protein

Alfredo De Lauro ^{†,1} Lorenzo Di Rienzo ^{†,* ,2} Mattia Miotto,² Pier Paolo Olimpieri,³ Edoardo Milanetti,^{3,2} and Giancarlo Ruocco^{2,3}

¹*Department of Sciences, Roma Tre University, 00146 Rome, Italy*

²*Center for Life Nano & Neuro-Science, Istituto Italiano di Tecnologia, Viale Regina Elena 291, 00161, Rome, Italy*

³*Department of Physics, Sapienza University, Piazzale Aldo Moro 5, 00185, Rome, Italy*

Many factors influence biomolecules binding, and its assessment constitutes an elusive challenge in computational structural biology. In this respect, the evaluation of shape complementarity at molecular interfaces is one of the main factors to be considered. We focus on the particular case of antibody-antigen complexes to quantify the complementarities occurring at molecular interfaces. We relied on a method we recently developed, which employs the 2D Zernike descriptors, to characterize investigated regions with an ordered set of numbers summarizing the local shape properties. Collected a structural dataset of antibody-antigen complexes, we applied this method and we statistically distinguished, in terms of shape complementarity, pairs of interacting regions from non-interacting ones. Thus, we set up a novel computational strategy based on *in-silico* mutagenesis of antibody binding site residues. We developed a Monte Carlo procedure to increase the shape complementarity between the antibody paratope and a given epitope on a target protein surface. We applied our protocol against several molecular targets in SARS-CoV-2 Spike protein, known to be indispensable for viral cell invasion. We, therefore, optimized the shape of template antibodies for the interaction with such regions. As the last step of our procedure, we performed an independent molecular docking validation of the results of our Monte Carlo simulations. We can therefore evaluate if the chemical properties of the introduced residues are compatible with the target region.

I. INTRODUCTION

Cellular functioning is widely dependent on processes occurring when biological molecules recognize each other and bind [1, 2]. In particular, the non-covalent protein-protein pairing proved to be essential in several biochemical pathways, ranging from biocatalysis to organism immunity or cell regulatory network construction [3, 4]. Not surprisingly, in the last decades, a very high effort has been devoted to developing computational tools for the structural characterization of protein-protein complexes. The aim of these methods are various, varying from binding site identification [5, 6] to binding affinity prediction [7, 8] or protein-protein docking guide [9–12].

In this scenario, the shape complementarity at the molecular interface is one of the most basic tasks to take into account [1, 13, 14]. Indeed, the evaluation of shape complementarity is essential for docking, both in terms of searching and evaluating the binding poses [2, 15–18], and represent one of the factors to take into account for binding site recognition [5, 6] or to assess the binding affinity [19].

In this work, we focused on Antibody-Antigen interactions, since these complexes represent a critical case of molecular recognition where interface shape complementarity level is similar to the typical protein-protein interfaces [17, 20]. Moreover, antibodies have been the object of extensive biomedical studies since their modular architecture facilitates the engineering of novel binding sites [21–23].

Among the wide variety of methods developed in the last years, using the Zernike polynomials to describe the geometrical properties of a molecular region and to evaluate the complementarity with a putative binding partner region is an effective and promising strategy [24–27]. Indeed, once extracted the molecular surface region, its geometrical properties are summarized through a set of numerical descriptors, namely the Zernike descriptors. The accuracy of the description is increased by enlarging the number of descriptors considered [28–30].

The main advantage of the Zernike formalism is that the molecular surface representation is invariant under protein rotation, constituting an absolute morphological characterization of the examined protein region. Therefore, the complementarity between two molecular regions is computed by comparing their Zernike descriptors, without the need for any preliminary superposition step[31, 32].

In the last decade, the Zernike approach, in its 3D version, has been widely applied for the analysis of biomolecules [24, 25, 27, 31–37], proving its efficacy in characterizing both global and local proteins properties.

[†] These authors contributes equally to this work.

^{*} Corresponding author:
lorenzo.dirienzo@iit.it

We recently developed a computational protocol that allows us to employ the 2D Zernike formalism to assess the shape complementarity observed in protein-protein interfaces [6]. The utilization of the 2D formalism allows to sensibly decrease the computational time needed to compute the shape descriptors without significant loss in description accuracy [38].

Here, we collected a structural dataset of antibody-protein complexes solved in x-ray crystallography. We studied the interface's shape complementarities through the application of our recently developed method based on 2D Zernike descriptors. We demonstrated that such a description can recognize with satisfying success the specific interaction from non-specific ones. Indeed, paratopes show a complementarity statistically higher toward their corresponding epitopes than toward epitopes belonging to other antigens.

Based on these results, we propose a new computational protocol that, for a given target protein region, optimizes the shape complementarity of an antibody toward that region. Indeed, once a target region, belonging to a protein antigen, is identified and characterized with its Zernike descriptors, we compared such region with the paratope of the antibodies in our dataset. Selecting as starting template the antibody that has the most complementary patch, we perform a Monte Carlo (MC) simulation for the optimization of the paratope structural conformation. Through extensive computational mutagenesis, substituting in each step an interacting antibody residue with a random one, we accept or reject each mutation according to the gain in shape complementarity, as evaluated by the Zernike method [37, 38].

In the current pandemic situation the interactions between SARS-CoV-2 Spike protein and human cellular receptors have been extensively studied through 2D Zernike polynomials formalism [39–42]. Despite the generality of such an approach, we selected as a target for the optimization protocol some surface regions of SARS-CoV-2 Spike protein. We discuss here the results we got, given the high interest generated on such a protein due to the pandemic situation. Indeed, elucidating the interaction mechanism between antibodies and viral proteins represents a fundamental element for developing new therapies.

II. RESULTS AND DISCUSSION

A. Description of Antibody-Antigen interface through Zernike Descriptors

In the present section, we discuss the results we obtained applying our recently developed computational protocol [6] on a structural dataset composed of 229 antibody-antigen complexes (See Methods).

In particular, we firstly identified for each complex the paratope (epitope) as the set of residues with at least one atom closer than 4 Å to any antigen (antibody) atom. Therefore, after separately computing the molecular surface [43] for both the proteins in interaction, we extracted the portions of the molecular surfaces relating to the binding site residues to properly characterize the shape of the interacting regions of antibodies and antigens (See Figure 1.A).

Once identified the interacting regions, we characterized them through the 2D Zernike polynomials, summarizing their geometrical properties in an ordered set of numerical descriptors (See Materials and Methods). By definition, two perfectly fitting surfaces are characterized by the same shape, meaning that, in principle, the difference between their Zernike descriptors is zero. Therefore, the shape complementarity between two molecular regions is compactly evaluated by such formalism. The lower is the distance between the Zernike descriptors, the higher is the shape complementarity between the corresponding protein regions [6, 38].

We described all the paratopes and epitopes in the dataset with the Zernike formalism. We thus defined the *specific complementarities* as the distances computed between interacting paratope-epitope pairs and the *non-specific complementarities* as the distances computed when two regions belonging to different complexes (therefore not evolved to interact with each other) are compared. In other words, dealing with N antibody-antigen complexes, the specific complementarity, C_s , is defined as:

$$D(p_i, e_j)|_{i=j} = \sqrt{\sum_{k=1}^{121} (p_i^k - e_j^k)^2}|_{i=j} \quad (1)$$

where D is the Euclidean distance between the vectors of the paratope (p_i) and epitope (e_i) Zernike descriptors. Since we expanded all the paratopes and epitopes to order 20, we dealt with 121 descriptors for each binding region. On the other hand, the non-specific complementarities, C_{ns} , can be computed as:

$$D(p_i, e_j)|_{i \neq j} = \sqrt{\sum_{k=1}^{121} (p_i^k - e_j^k)^2}|_{i \neq j} \quad (2)$$

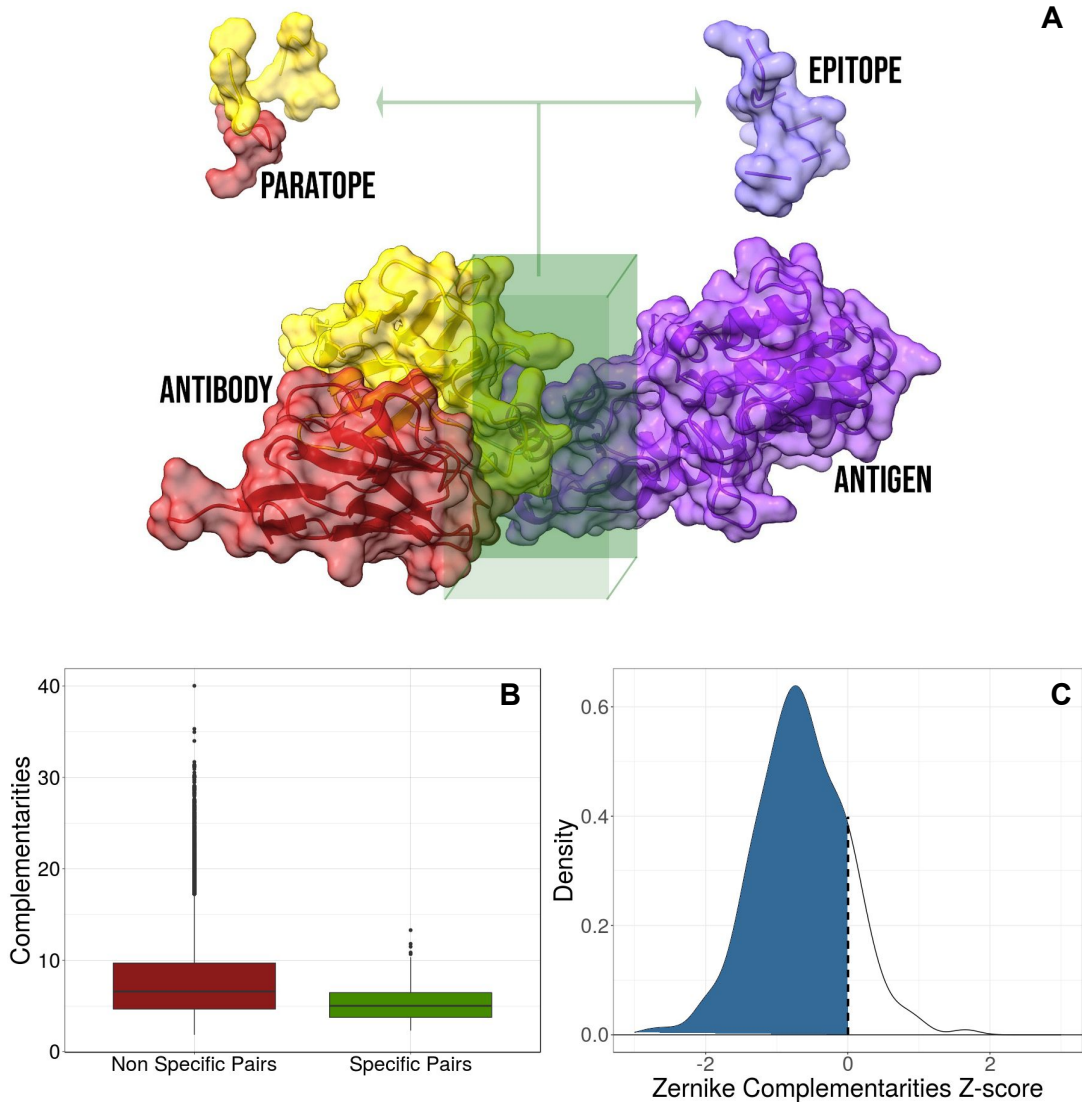


FIG. 1: Application of the 2D Zernike polynomials approach to antibody-antigen complexes. A) Representation of a generic molecular antibody-antigen complex: the antibody heavy chain, antibody light chain, and the antigen are in red, yellow, and purple, respectively. The interacting regions, defined as the portion of the molecular surfaces belonging to residues closer than 4 \AA to any atoms of the molecular partner, are extracted from the whole surface. B) Boxplot comparing the *specific complementarity*, i.e. the complementarity between regions actually found in interaction (green), and the *non-specific complementarity*, i.e. the complementarity observed between paratopes and epitopes of different complexes (red). It is worth remarking that when the numerical value is low, the complementarity is high. C) Z-scores distribution of the specific complementarity. When the Z-score is lower than 0, the specific interaction is characterized by a complementarity higher than the mean of the non-specific interaction.

In Figure 1.B we reported a boxplot highlighting the differences between C_s and C_{ns} distributions. As expected, the distribution of C_s is statistically lower than the distribution of C_{ns} (Kolmogorov-Smirnov test p -value $< 2.2e-16$), testifying the sensitivity of Zernike in recognizing regions actually in contact from non-interacting ones. As the second step, we normalized the Zernike complementarities with the Z-score. In particular, for each paratope we have 1 C_s and 228 C_{ns} complementarity values, each of which is related to a specific patch pair. Normalizing over this set of numbers and looking at the Z-score regarding the specific one, we assessed the propensity that characterizes each antibody toward its specific antigen. In Figure 1.C we report the distribution of such specific Z-scores. As evident, they are mostly negatives (86% of the cases have Z-score lower than 0, 28% have Z-score lower than -1), providing evidence that specific interactions are characterized by lower distances (higher complementarity) than non-specific ones.

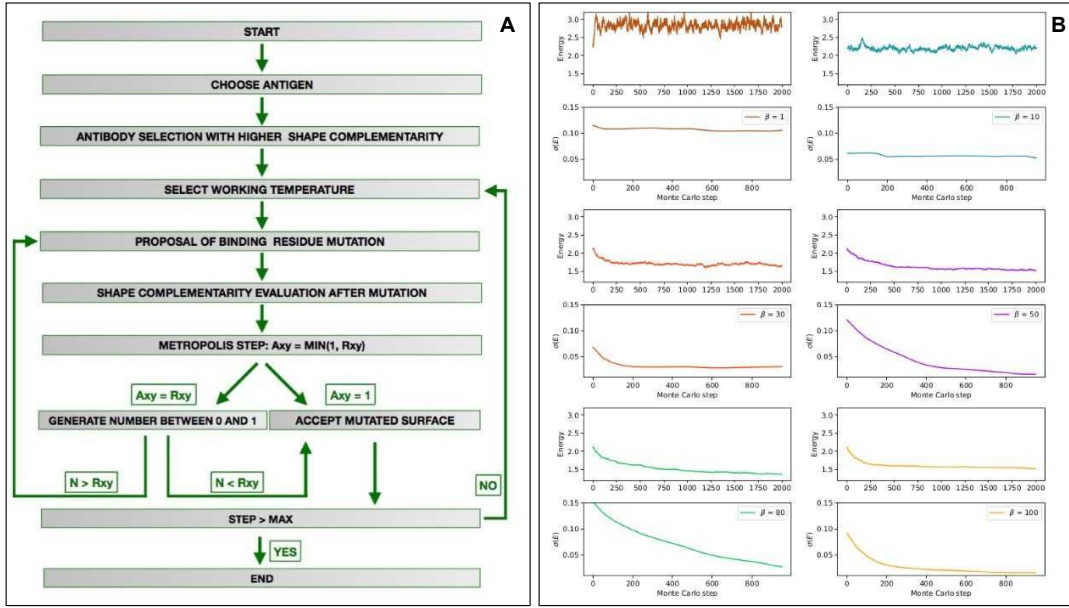


FIG. 2: **Development of a Monte Carlo for shape complementarity optimization against a target region.** **A)** Flowchart depicting the main steps of the computational protocol we developed. **B)** Results of the mutagenesis Monte Carlo procedures performed at fixed β ($\beta = 1, 10, 30, 50, 80, 100$). The top panels represent the energy (i.e. the shape complementarity) as a function of the Monte Carlo steps. The low panels show the standard deviation of energy of the remaining part of the Monte Carlo simulations as a function of the Montecarlo steps (i.e. $\sigma(E)$ for $n = 1000$ means standard deviations of the energy obtained in the steps 1001-2000).

Taken together, these results confirm the ability of our method to correctly capture the main determinant of molecular shape complementarity.

B. Zernike based Monte Carlo simulation for molecular interface optimization

The Zernike formalism enjoys several advantageous features in representing molecular surface: mainly, the invariance under rotation that makes such descriptors an "absolute" characterization of local protein morphology and the low computational cost of its calculation. Indeed, in this section, we present our algorithm that, exploiting these advantages, aims to optimize the shape complementarity of an antibody toward a given molecular target region. A similar procedure has already been presented and tested in our previous work [37], and here for the first time it is applied to antibody-antigen interaction systems.

Figure 2.A illustrates the main steps of the algorithm. We defined the target region as the portion of the antigen surface toward which an antibody will be optimized. It is thus necessary to identify the antibody chosen as a starting point of the algorithm. Summarized with the Zernike descriptors the target region we compute the shape complementarity with all the paratope of our dataset: here, the template, i.e. the antibody selected as the starting point for the mutagenesis process, can be chosen among the paratopes characterized by a high initial complementarity.

Established the template, we perform a Monte Carlo simulation employing computational mutagenesis on the paratope residues. In each step, we randomly select a residue mutating it in another of the 19 possible ones. The mutation generates a different paratope, characterized by a different shape of its molecular surface. Consequently, recomputing the Zernike descriptors we can evaluate the effect of the mutation on the complementarity with the target region: indeed we can define the *complementarity balance* as:

$$\Delta C = C_{mut} - C_{wt} = D(p_{mut}, e_{tar}) - D(p_{orig}, e_{tar}) \quad (3)$$

where p_{orig} and p_{mut} are the Zernike descriptors of the original and the mutated paratope respectively, while the e_{tar} represent the Zernike descriptors of the target epitope and D represent the distance between 2 sets of descriptors. Since, as said, a high complementarity is reached when D is low, $\Delta C < 0$ means a higher complementary surface, and $\Delta C > 0$ is obtained when the mutation is deleterious since it causes a worsening of the shape complementarity.

The number of combinations of possible mutations in an interacting region, composed usually of tens of residues, is huge. Therefore, to effectively sample the space of the possible mutants, we perform a Monte Carlo Metropolis simulation, iterating the procedure described above, where the mutation in each step is accepted according to the following rules:

$$P = \begin{cases} 1 & \text{if } \Delta C < 0 \\ e^{-\beta \Delta C} & \text{if } \Delta C \geq 0 \end{cases} \quad (4)$$

where β is the temperature factor that determines the probability of acceptance of a step worsening complementarity. Note that this aspect is crucial to properly explore a large number of different mutants: β is thus progressively decreased during the Monte Carlo simulation, progressively confining the system in an energy minimum in a simulated annealing process [44].

To observe how many steps are necessary to reach the equilibrium for each β , we preliminary ran several fixed-temperature Monte Carlo simulations. We selected the epitope of an antigen structure in our dataset (PDB id: 1AR1) and, excluding its own one, we choose as the starting template the most complementary paratope in the structural dataset. We thus performed six different Monte Carlo simulations, each for a different β , where the acceptance probability in each mutagenesis step is given by Eq. 4. Performing 10 independent simulations of $N = 2000$ steps for each β , the averaged results we obtained are summarized in Figure 2.B. In the top panels, we reported the energy (i.e. the complementarity) as a function of the Monte Carlo steps. In the low panels, we reported the standard deviation of the energy of the remaining part of the Monte Carlo simulations as a function of the number of steps (i.e. $\sigma(E)$ for $n=1000$ means standard deviations of the energy obtained in the steps 1001-2000). As expected, for low values of β (i.e. high temperature) the system lives in a condition of indifferent equilibrium, where whatever mutation has an equal likelihood to be accepted, independently from its effect on complementarity. When, on the contrary, β is high, the energy of the system rapidly decreases to a stationary local minimum. This trend is confirmed by looking at the stationary value of energies or, equivalently, noting that standard deviation tends progressively to zero. In the light of these results, in our protocol, we set $N = 700$ for each temperature. In this way, we preliminary allow the system to move away from the starting local conformation, thus freezing it in a new energy minimum, characterized by an increased shape complementarity with the target region.

C. A Case of Study: Application to SARS-CoV-2 Spike Protein

The approach described here is general and can be applied to whatever protein. This notwithstanding, we applied it to the SARS-CoV-2 spike protein, a very relevant case of macromolecular interaction. Indeed, the severe acute respiratory syndrome coronavirus 2 infection is still causing very serious danger for public health [45, 46].

Many therapeutic strategies are devoted to SARS-CoV-2 Spike protein, protruding from the viral envelope and responsible for cell entry mechanism [47–49]. In this framework, we selected on spike molecular surfaces three different regions as targets for the optimization protocol. On one hand, we targeted the two different molecular regions involved in the interaction between Spike and angiotensin-converting enzyme 2 (ACE-2), the well-known cellular receptor responsible for viral cell invasion. Moreover, we optimized an antibody also toward a very exposed region in the N-terminal Spike domain, responsible for contacting sialic acid molecules. Indeed, such interaction can confer to the virus, as occur for the Middle East respiratory syndrome coronavirus (MERS-CoV) [50], an additional molecular mechanism for cell intrusion. The responsible Spike region represents a promising therapeutic target [39, 51].

We selected the residues constituting such epitopes and we characterized their molecular surfaces through Zernike formalism. Thus, we calculated the complementarity between these regions and all the antibody binding sites in our dataset. To begin the optimization from a favorite starting point, we selected as templates antibody binding sites characterized by the highest complementarity with each identified target.

We applied the procedure described in the previous section obtaining optimized paratopes whose molecular images are shown in Figure 3.A, where we reported both the optimized antibodies and antigen interacting surfaces. In Figure 3.B, we reported, for each of the Monte Carlo simulations performed, the shape complementarity as a function of the steps of the simulation, where the dashed lines enclose ranges with different β values. Each simulation significantly optimizes shape complementarity, obtaining a Zernike distance decrease of 43%, on average. Significantly, all the designed binding sites are characterized by a very high final shape complementarity, in terms of Zernike descriptors. Indeed, it is worth noting that the values obtained by all the three designed binding sites are lower than all the specific complementarities obtained in our structural dataset.

The computational protocol we developed does not take into account several properties, known to be important in molecular recognition, such as electrostatics or hydrophobicity. In particular, our working hypothesis is that the shape

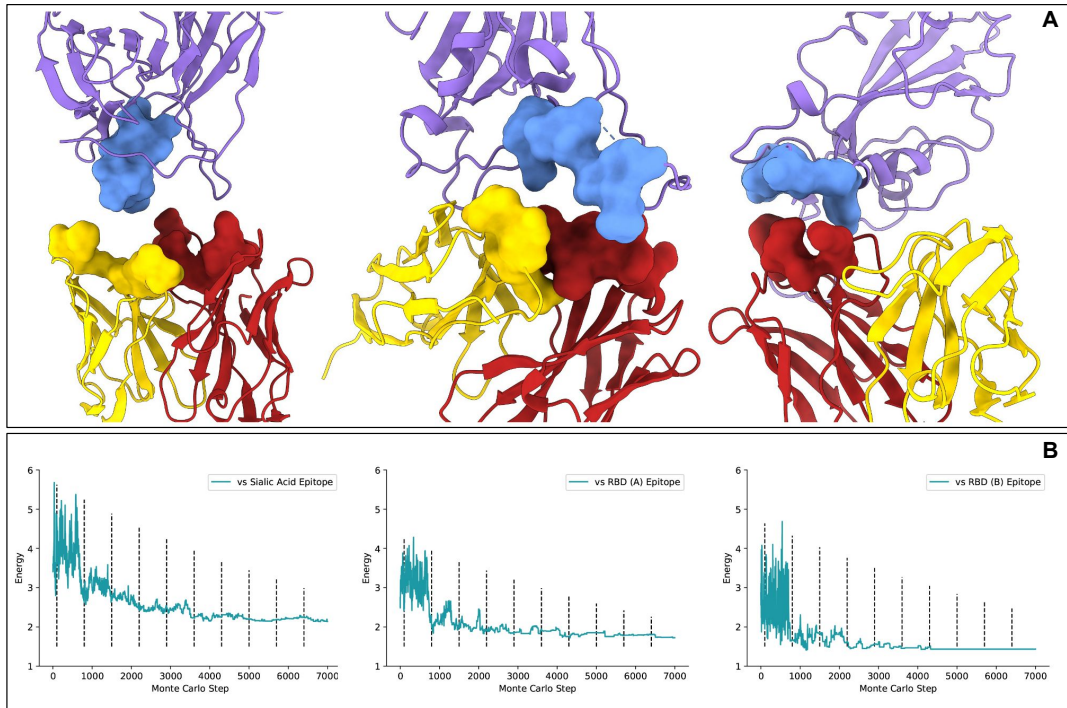


FIG. 3: **Application of the optimization protocol to SARS-CoV-2 Spike protein.** **A)** Molecular representation of the optimized antibodies binding epitopes on Spike protein. The antibody light and heavy chains are shown in yellow and red respectively, while the antigen is in purple. **B)** Shape complementarity as a function of the Monte Carlo steps for all the antibodies we optimized. Dashed lines separate different temperature intervals of the simulations.

complementarity plays a primary role as a perfect match between molecular surfaces is due to an optimal structural rearrangement, which is probably caused by the compatibility of amino acid compositions of the interacting patches. However, the relationship between shape complementarity and chemical-physical properties is not always trivial, requiring a further test for the patches proposed as interacting, to also analyze the compatibility of a chemical nature. This means that a residue substitution can in principle worsen the chemical compatibility between molecules, even if the shape complementarity is enhanced. For this reason, as a further step of our optimization protocol, we performed a molecular docking analysis using HDOCK [12]. More specifically, we docked Spike protein and the antibodies, both in the original and in the optimized versions, to study the effects our computational protocol has produced. We constrained docking to interact with the residues composing the Spike target epitopes and the antibodies optimized regions. We summarized in Figure 4 the results we obtained.

Thus, we selected the 10 best docking poses regarding both the original and the optimized antibodies. To assess whether the optimization protocol has been effective, some estimators of binding compatibility have been calculated. In particular, the number of residue-residue inter-molecular contacts, the surface buried in the complex, and the mean distance of the closest atoms between the two interfaces. For each of these observables, we computed the relative percentage of gaining after optimization so as positive values indicate an increased binding tightness (See Materials and Methods). As shown in Figure 4.A, even if in two applications we note a worsening, in one case the optimization procedure has produced an antibody with better values of all such estimators, indicating the importance of including the molecular docking approach as a filter of selected patches based on geometric compatibility.

We focused therefore on this case and we analyzed how the introduced residue substitutions caused this augment. Analyzing the best docking poses, in Figure 4.B we reported the gaining in terms of the number of inter-molecular contacts each residue registered before and after the optimization. Each residue is represented by a blue bar, while the residues mutated in the protocol are depicted in orange. As evident, the main effect regarding the residues "H 31" and "H 32". Indeed, to increase the shape complementarity, the optimization protocol preferred to switch the exposition of these residues. Interestingly, the principal increasing inter-molecular contacts are concentrated in residues close to the mutated ones, underlying the capability of the protocol to modify the binding area as a whole.

Lastly, we assessed the difference in residue-residue inter-molecular interaction networks. In Figure 4.C we reported the contacts between the main couples of residues, where a higher number of occurrences in the docking poses is testified by the thickness and the color of the edge. The Spike residues are shown in green, the antibody ones are in

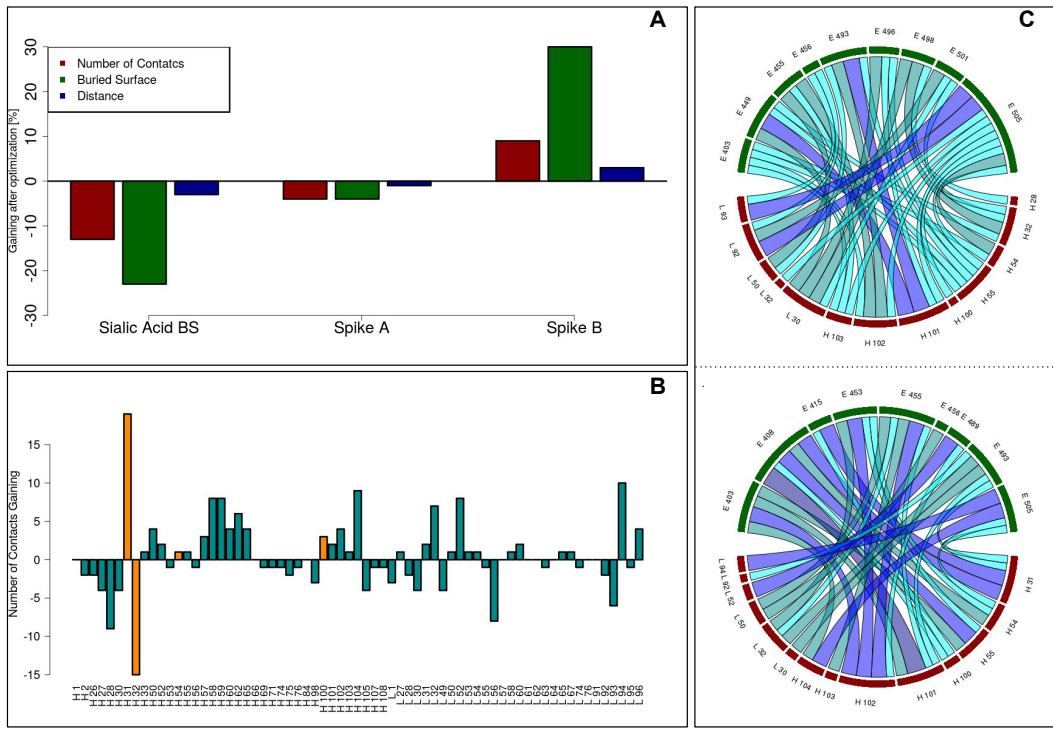


FIG. 4: Results of the docking analysis.. **A)** Each bar represents the relative gaining (in terms of the number of residue-residue inter-molecular contacts, the surface buried in the complex, and the mean inter-molecular distance of the closest atoms) between the 10 best docking poses obtained with the original and the optimized antibodies. A positive value means an increase in binding compatibility. **B)** The gaining in terms of the number of inter-molecular contacts each residue registered before and after the optimization. **C)** The network of residue-residue interactions at the interface when the original (upper figure) or the optimized (lower figure) are docked to Spike B region. The color, from cyan to dark blue, and the width of the edges reflect the occurrences in the docking poses of a given contact.

red. As further proof of the goodness of the proposed mutants, it can be noted that the interface of the optimized antibody (lower figure) is much more interconnected than the one of the original antibody (upper figure), indicating a possible effect on binding stability.

III. CONCLUSIONS

The binding affinity between biomolecules depends on a complex balance of several effects, including enthalpic and entropic contributions. Indeed, the substitution of even one residue at the interface could produce dramatic changes. Although many efforts were spent in this direction, predicting such effects has proven to be a difficult task and is still an open problem in computational biology.

In this scenario, the evaluation of shape complementarity between molecular regions is undoubtedly a central aspect. In this work, we focused on antibody-antigen interaction, a relevant case of molecular recognition. We applied our recently developed formalism based on the 2D Zernike polynomials to evaluate the shape complementarity with a quantitative approach. Once summarized the topological properties of interacting regions with a set of numerical descriptors, we demonstrated that such formalism assigns to pairs of interacting regions complementarities statistically higher than the ones assigned to regions not in interaction.

We thus developed a Monte Carlo based approach for the shape optimization of an antibody towards a molecular target region. We propose a new strategy that, potentially, can identify the antibody with the highest shape complementarity for a given epitope of any antigen protein.

Because of the emergence of viral variants that can eventually escape antibodies matured in vaccinated or recovered patients, the interactions between antibodies and SARS-CoV-2 Spike protein are being extensively studied and still needs further investigation.

For this reason, we selected three molecular regions on Spike protein as the target epitopes for our procedure. We, therefore, devised a set of antibodies characterized by a high shape complementarity toward their cognate epitopes.

Still, chemical characteristics of inserted residues were not considered in this optimization procedure, as well as entropic balance or immunoglobulin fold constraints. Therefore, after the inclusion of terms accounting for other aspects of binding compatibility in the Monte Carlo, this procedure can represent a promising strategy for interface region molecular design. In the present work, we highlighted with an independent molecular docking evaluation the case when the optimization procedure has increased molecular complex compactness.

IV. MATERIALS AND METHODS

A. Dataset

We selected 229 protein-binding antibodies with sequence identity lower than 90% and resolution $< 3.0 \text{ \AA}$ using the SabDab database [52]. The sequence of each antibody was renumbered according to the Chothia numbering scheme [53, 54] using an in-house python script.

The structure of SARS-CoV-2 Spike protein used for the identification of ACE2 interacting region have the pdb code 6vw1. When we investigated the N-terminal domain we used the structure 7jji.

We identified on Spike protein two epitopes in the ACE2 binding region: Spike A and Spike B. Spike A epitope is constituted by the residues: "TYR 453, LEU 455, PHE 456, ALA 475, GLY 476, PHE 486, ASN 487, TYR 489, GLN 493". Spike B epitope is constituted by the residues: "TYR 449, GLY 496, GLN 498, THR 500, ASN 501, GLY 502, TYR 505". We identified another epitope in the N-terminal domain, in the region involved in sialic acid binding. That region is defined as the set of residues whose CA atoms are closer than 8 \AA to the TRP 258 CA [39]. Such epitope is constituted by these residues: "LEU 244, HIS 245, ARG 246, SER 247, TYR 248, LEU 249, THR 250, PRO 251, GLY 252, ASP 253, SER 254, SER 255, SER 256, GLY 257, TRP 258, THR 259, ALA 260".

B. Surface Construction

Using as reference the experimental structures, computational mutagenesis has been performed using SCWRL4 [55].

For each protein structure, Solvent Accessible Surface is computed using DMS software with standard option [43]. The interacting surface is constituted by the surface points belonging to interacting residues, defined as the set of residues having at least one atom closer than 4 \AA to any atoms of the molecular partner.

C. Zernike Descriptors

Given a 2D function $f(r, \phi)$ in the unitary circle(region $r < 1$), it can be expanded in the Zernike polynomials basis. Therefore:

$$f(r, \phi) = \sum_{n=0}^{\infty} \sum_{m=0}^{m=n} c_{nm} Z_{nm} \quad (5)$$

where

$$\begin{aligned} c_{nm} &= \frac{(n+1)}{\pi} \langle Z_{nm} | f \rangle = \\ &= \frac{(n+1)}{\pi} \int_0^1 dr r \int_0^{2\pi} d\phi Z_{nm}^*(r, \phi) f(r, \phi) \end{aligned} \quad (6)$$

are the expansion coefficients (Zernike moments). The complex functions $Z_{nm}(r, \phi)$ are the Zernike polynomials, each composed by a radial and an angular part:

$$Z_{nm} = R_{nm}(r) e^{im\phi}. \quad (7)$$

The radial dependence, given n and m , can be written as follow:

$$R_{nm}(r) = \sum_{k=0}^{\frac{n-m}{2}} \frac{(-1)^k (n-k)!}{k! (\frac{n+m}{2} - k)! (\frac{n-m}{2} - k)!} r^{n-2k} \quad (8)$$

For each couple of polynomials, this rule holds:

$$\langle Z_{nm} | Z_{n'm'} \rangle = \frac{\pi}{(n+1)} \delta_{nn'} \delta_{mm'} \quad (9)$$

Therefore the set of polynomials forms a basis. Knowing the coefficients, $\{c_{nm}\}$ allows the reconstruction of the original function. The level of the detail can be modified by modulating the order of expansion, $N = \max(n)$.

The norm of each coefficient ($z_{nm} = |c_{nm}|$) does not depend on the phase, therefore it is invariant under rotations around the origin.

The shape complementarity between two regions can be evaluated by comparing their Zernike invariants. In particular, we measured the complementarity between region i and j as the Euclidean distance between the invariant vectors, i.e.

$$d_{ij} = \sqrt{\sum_{k=1}^{M=121} (z_i^k - z_j^k)^2} \quad (10)$$

We adopted $N=20$, therefore dealing with 121 invariant descriptors for each patch.

D. Analysis of docking poses

We docked the three original and the three optimized antibody structures with spike using HDOCK[12], indicating as interacting residues the one written in Dataset section.

We selected, for all the 6 docking simulations, the best 10 poses. For each pose we calculated:

- the number of inter-molecular residue-residue contacts. Two residues are in contact if the minimum distance between their atoms is less than 4 Å.
- the surface buried in the complex. The surface buried is defined as the difference between the sum of the monomers' area and the complex area.
- the mean of the lowest 100 atom-atom inter-molecular distances.

The comparison between the results regarding original and optimized antibodies are performed so as a positive value means an increasing in binding compatibility after optimization. Therefore the relative percentage of gaining is defined as:

- Number of contacts : $\frac{\langle Cont \rangle_{opt} - \langle Cont \rangle_{orig}}{\langle Cont \rangle_{orig}}$
- Buried Area : $\frac{\langle Surf \rangle_{opt} - \langle Surf \rangle_{orig}}{\langle Surf \rangle_{orig}}$
- Distance : $\frac{\langle Dist \rangle_{orig} - \langle Dist \rangle_{opt}}{\langle dist \rangle_{orig}}$

where the subscripts "orig" and "opt" refer to the poses obtained with antibodies before and after the optimization, respectively.

Data Availability Statement

All the molecular structures used for this work are available on Protein Data Bank (<https://www.rcsb.org/>).

Conflict of Interest Disclosure

The authors declare no conflicts of interests.

Acknowledgments

The research leading to these results has been also supported by European Research Council Synergy grant ASTRA (n. 855923).

[1] Susan Jones and Janet M Thornton. Principles of protein-protein interactions. *Proceedings of the National Academy of Sciences*, 93(1):13–20, 1996.

[2] M Michael Gromiha, K Yugandhar, and Sherlyn Jemimah. Protein–protein interactions: scoring schemes and binding affinity. *Current opinion in structural biology*, 44:31–38, 2017.

[3] Anne-Claude Gavin, Markus Bösche, Roland Krause, Paola Grandi, Martina Marzioch, Andreas Bauer, Jörg Schultz, Jens M Rick, Anne-Marie Michon, Cristina-Maria Cruciat, et al. Functional organization of the yeast proteome by systematic analysis of protein complexes. *Nature*, 415(6868):141–147, 2002.

[4] Jing-Dong J Han, Nicolas Bertin, Tong Hao, Debra S Goldberg, Gabriel F Berrez, Lan V Zhang, Denis Dupuy, Albertha JM Walhout, Michael E Cusick, Frederick P Roth, et al. Evidence for dynamically organized modularity in the yeast protein–protein interaction network. *Nature*, 430(6995):88–93, 2004.

[5] Pablo Gainza, Freyr Sverrisson, Frederico Monti, Emanuele Rodola, D Boscaini, MM Bronstein, and BE Correia. Deciphering interaction fingerprints from protein molecular surfaces using geometric deep learning. *Nature Methods*, 17(2):184–192, 2020.

[6] Edoardo Milanetti, Mattia Miotto, Lorenzo Di Rienzo, Michele Monti, Giorgio Gosti, and Giancarlo Ruocco. 2d zernike polynomial expansion: Finding the protein-protein binding regions. *Computational and structural biotechnology journal*, 19:29–36, 2021.

[7] Till Siebenmorgen and Martin Zacharias. Computational prediction of protein–protein binding affinities. *Wiley Interdisciplinary Reviews: Computational Molecular Science*, 10(3):e1448, 2020.

[8] Anna Vangone and Alexandre MJJ Bonvin. Contacts-based prediction of binding affinity in protein–protein complexes. *elife*, 4:e07454, 2015.

[9] Ilya A Vakser. Protein-protein docking: From interaction to interactome. *Biophysical journal*, 107(8):1785–1793, 2014.

[10] Dima Kozakov, David R Hall, Bing Xia, Kathryn A Porter, Dzmitry Padhorny, Christine Yueh, Dmitri Beglov, and Sandor Vajda. The cluspro web server for protein–protein docking. *Nature protocols*, 12(2):255, 2017.

[11] Cunliang Geng, Yong Jung, Nicolas Renaud, Vasant Honavar, Alexandre MJJ Bonvin, and Li C Xue. iscore: a novel graph kernel-based function for scoring protein–protein docking models. *Bioinformatics*, 36(1):112–121, 2020.

[12] Yumeng Yan, Huanyu Tao, Jiahua He, and Sheng-You Huang. The hdock server for integrated protein–protein docking. *Nature protocols*, 15(5):1829–1852, 2020.

[13] Ephraim Katchalski-Katzir, Isaac Shariv, Miriam Eisenstein, Asher A Friesem, Claude Aflalo, and Ilya A Vakser. Molecular surface recognition: determination of geometric fit between proteins and their ligands by correlation techniques. *Proceedings of the National Academy of Sciences*, 89(6):2195–2199, 1992.

[14] Michael C Lawrence and Peter M Colman. Shape complementarity at protein/protein interfaces, 1993.

[15] Rong Chen and Zhiping Weng. A novel shape complementarity scoring function for protein-protein docking. *Proteins: Structure, Function, and Bioinformatics*, 51(3):397–408, 2003.

[16] George Nicola and Ilya A Vakser. A simple shape characteristic of protein–protein recognition. *Bioinformatics*, 23(7):789–792, 2007.

[17] Daisuke Kuroda and Jeffrey J Gray. Shape complementarity and hydrogen bond preferences in protein–protein interfaces: implications for antibody modeling and protein–protein docking. *Bioinformatics*, 32(16):2451–2456, 2016.

[18] Yumeng Yan and Sheng-You Huang. Pushing the accuracy limit of shape complementarity for protein-protein docking. *BMC bioinformatics*, 20(25):1–10, 2019.

[19] Ariel Erijman, Eran Rosenthal, and Julia M Shifman. How structure defines affinity in protein-protein interactions. *PLOS one*, 9(10):e110085, 2014.

[20] Yili Li, Hongmin Li, Feng Yang, Sandra J Smith-Gill, and Roy A Mariuzza. X-ray snapshots of the maturation of an antibody response to a protein antigen. *Nature Structural & Molecular Biology*, 10(6):482–488, 2003.

[21] Surjit Singh, Nitish K Tank, Pradeep Dwiwedi, Jaykaran Charan, Rimplejeet Kaur, Preeti Sidhu, and Vinay K Chugh. Monoclonal antibodies: a review. *Current clinical pharmacology*, 13(2):85–99, 2018.

[22] Abdullah FUH Saeed, Rongzhi Wang, Sumei Ling, and Shihua Wang. Antibody engineering for pursuing a healthier future. *Frontiers in microbiology*, 8:495, 2017.

[23] Philip Gotwals, Scott Cameron, Daniela Cipolletta, Viviana Cremasco, Adam Crystal, Becker Hewes, Britta Mueller, Sonia Quaratino, Catherine Sabatos-Peyton, Lilli Petruzzelli, et al. Prospects for combining targeted and conventional cancer therapy with immunotherapy. *Nature Reviews Cancer*, 17(5):286–301, 2017.

[24] Vishwesh Venkatraman, Lee Sael, and Daisuke Kihara. Potential for protein surface shape analysis using spherical harmonics and 3d zernike descriptors. *Cell biochemistry and biophysics*, 54(1-3):23–32, 2009.

[25] Lorenzo Di Rienzo, Edoardo Milanetti, Rosalba Lepore, Pier Paolo Olimpieri, and Anna Tramontano. Superposition-free comparison and clustering of antibody binding sites: implications for the prediction of the nature of their antigen. *Scientific reports*, 7(1):1–10, 2017.

[26] Lorenzo Di Rienzo, Edoardo Milanetti, Giancarlo Ruocco, and Rosalba Lepore. Quantitative description of surface complementarity of antibody-antigen interfaces. *Frontiers in molecular biosciences*, page 933, 2021.

[27] Sebastian Daberdaku and Carlo Ferrari. Antibody interface prediction with 3d zernike descriptors and svm. *Bioinformatics*, 35(11):1870–1876, 2019.

[28] Frits Zernike. Diffraction theory of the knife-edge test and its improved form, the phase-contrast method. *Monthly Notices of the Royal Astronomical Society*, 94:377–384, 1934.

[29] Marcin Novotni and Reinhard Klein. Shape retrieval using 3d zernike descriptors. *Computer-Aided Design*, 36(11):1047–1062, 2004.

[30] N Canterakis. 3d zernike moments and zernike affine invariants for 3d image analysis and recognition. In *In 11th Scandinavian Conf. on Image Analysis*. Citeseer, 1999.

[31] Sebastian Daberdaku and Carlo Ferrari. Exploring the potential of 3d zernike descriptors and svm for protein–protein interface prediction. *BMC bioinformatics*, 19(1):35, 2018.

[32] Lorenzo Di Rienzo, Edoardo Milanetti, Josephine Alba, and Marco D’Abramo. Quantitative characterization of binding pockets and binding complementarity by means of zernike descriptors. *Journal of Chemical Information and Modeling*, 60(3):1390–1398, 2020.

[33] Vishwesh Venkatraman, Yifeng D Yang, Lee Sael, and Daisuke Kihara. Protein-protein docking using region-based 3d zernike descriptors. *BMC bioinformatics*, 10(1):407, 2009.

[34] Daisuke Kihara, Lee Sael, Rayan Chikhi, and Juan Esquivel-Rodriguez. Molecular surface representation using 3d zernike descriptors for protein shape comparison and docking. *Current Protein and Peptide Science*, 12(6):520–530, 2011.

[35] Josephine Alba, Lorenzo Di Rienzo, Edoardo Milanetti, Oreste Acuto, and Marco D’Abramo. Molecular dynamics simulations reveal canonical conformations in different pmhc/tcr interactions. *Cells*, 9(4):942, 2020.

[36] Xusi Han, Atilla Sit, Charles Christoffer, Siyang Chen, and Daisuke Kihara. A global map of the protein shape universe. *PLoS computational biology*, 15(4):e1006969, 2019.

[37] Lorenzo Di Rienzo, Edoardo Milanetti, Claudia Testi, Linda Celeste Montemiglio, Paola Baiocco, Alberto Boffi, and Giancarlo Ruocco. A novel strategy for molecular interfaces optimization: The case of ferritin-transferrin receptor interaction. *Computational and structural biotechnology journal*, 18:2678–2686, 2020.

[38] Lorenzo Di Rienzo, Michele Monti, Edoardo Milanetti, Mattia Miotto, Alberto Boffi, Gian Gaetano Tartaglia, and Giancarlo Ruocco. Computational optimization of angiotensin-converting enzyme 2 for sars-cov-2 spike molecular recognition. *Computational and Structural Biotechnology Journal*, 2021.

[39] Edoardo Milanetti, Mattia Miotto, Lorenzo Di Rienzo, Madhu Nagaraj, Michele Monti, Thaddeus W. Golbek, Giorgio Gosti, Steven J. Roeters, Tobias Weidner, Daniel E. Otzen, and Giancarlo Ruocco. In-silico evidence for a two receptor based strategy of SARS-CoV-2. *Frontiers in Molecular Biosciences*, 8, June 2021.

[40] Mattia Miotto, Lorenzo Di Rienzo, Leonardo Bò, Alberto Boffi, Giancarlo Ruocco, and Edoardo Milanetti. Molecular mechanisms behind anti SARS-CoV-2 action of lactoferrin. *Frontiers in Molecular Biosciences*, 8, February 2021.

[41] Leonardo Bò, Mattia Miotto, Lorenzo Di Rienzo, Edoardo Milanetti, and Giancarlo Ruocco. Exploring the association between sialic acid and sars-cov-2 spike protein through a molecular dynamics-based approach. *Frontiers in medical technology*, page 24, 2021.

[42] Mattia Miotto, Lorenzo Di Rienzo, Giorgio Gosti, Leonardo Bo, Giacomo Parisi, Roberta Piacentini, Alberto Boffi, Giancarlo Ruocco, and Edoardo Milanetti. Inferring the stabilization effects of sars-cov-2 variants on the binding with ace2 receptor. *Communications Biology*, 5(1):1–13, 2022.

[43] Frederic M Richards. Areas, volumes, packing, and protein structure. *Annual review of biophysics and bioengineering*, 6(1):151–176, 1977.

[44] Scott Kirkpatrick, C Daniel Gelatt, and Mario P Vecchi. Optimization by simulated annealing. *science*, 220(4598):671–680, 1983.

[45] Chaolin Huang, Yeming Wang, Xingwang Li, Lili Ren, Jianping Zhao, Yi Hu, Li Zhang, Guohui Fan, Jiuyang Xu, Xiaoying Gu, et al. Clinical features of patients infected with 2019 novel coronavirus in wuhan, china. *The Lancet*, 395(10223):497–506, 2020.

[46] Na Zhu, Dingyu Zhang, Wenling Wang, Xingwang Li, Bo Yang, Jingdong Song, Xiang Zhao, Baoying Huang, Weifeng Shi, Roujian Lu, et al. A novel coronavirus from patients with pneumonia in china, 2019. *New England Journal of Medicine*, 2020.

[47] Peng Zhou, Xing-Lou Yang, Xian-Guang Wang, Ben Hu, Lei Zhang, Wei Zhang, Hao-Rui Si, Yan Zhu, Bei Li, Chao-Lin Huang, et al. A pneumonia outbreak associated with a new coronavirus of probable bat origin. *Nature*, pages 1–4, 2020.

[48] Alexandra C Walls, Young-Jun Park, M Alejandra Tortorici, Abigail Wall, Andrew T McGuire, and David Veesler. Structure, function, and antigenicity of the sars-cov-2 spike glycoprotein. *Cell*, 2020.

[49] Yushun Wan, Jian Shang, Rachel Graham, Ralph S Baric, and Fang Li. Receptor recognition by novel coronavirus from wuhan: An analysis based on decade-long structural studies of sars. *Journal of virology*, 2020.

[50] Wentao Li, Ruben JG Hulswit, Ivy Widjaja, V Stalin Raj, Ryan McBride, Wenjie Peng, Widagdo Widagdo, M Alejandra Tortorici, Brenda Van Dieren, Yifei Lang, et al. Identification of sialic acid-binding function for the middle east respiratory syndrome coronavirus spike glycoprotein. *Proceedings of the National Academy of Sciences*, 114(40):E8508–E8517, 2017.

[51] Alexander N Baker, Sarah-Jane Richards, Collette S Guy, Thomas R Congdon, Muhammad Hasan, Alexander J Zwetsloot, Angelo Gallo, Józef R Lewandowski, Phillip J Stansfeld, Anne Straube, et al. The sars-cov-2 spike protein binds sialic acids and enables rapid detection in a lateral flow point of care diagnostic device. *ACS central science*, 6(11):2046–2052, 2020.

[52] James Dunbar, Konrad Krawczyk, Jinwoo Leem, Terry Baker, Angelika Fuchs, Guy Georges, Jiye Shi, and Charlotte M

Deane. Sabdab: the structural antibody database. *Nucleic acids research*, 42(D1):D1140–D1146, 2013.

[53] Cyrus Chothia and Arthur M Lesk. Canonical structures for the hypervariable regions of immunoglobulins. *Journal of molecular biology*, 196(4):901–917, 1987.

[54] Cyrus Chothia, Arthur M Lesk, Anna Tramontano, Michael Levitt, Sandra J Smith-Gill, Gillian Air, Steven Sheriff, Eduardo A Padlan, David Davies, William R Tulip, et al. Conformations of immunoglobulin hypervariable regions. *Nature*, 342(6252):877, 1989.

[55] Georgii G Krivov, Maxim V Shapovalov, and Roland L Dunbrack Jr. Improved prediction of protein side-chain conformations with scwrl4. *Proteins: Structure, Function, and Bioinformatics*, 77(4):778–795, 2009.